J. Membrane Biol. 62, 139–148 (1981)

The Journal of
Membrane Biology

# Current-Voltage Curve of Electrogenic $Cl^-$ Pump Predicts Voltage-Dependent $Cl^-$ Efflux in *Acetabularia*

H. Mummert, U.-P. Hansen*, and D. Gradmann**

Institut für Biologie I, Auf der Morgenstelle 1, D-7400 Tübingen, West Germany

**Summary.** The current-voltage relationship of carrier-mediated, passive and active ion transport systems with one charge-carrying pathway can exactly be described by a simple reaction kinetic model. This model consists of two carrier states (one inside, one outside) and two pairs (forwards and backwards) of rate constants: a voltage-dependent one, describing the transport of charge and a voltage-insensitive one, summarizing all the other (voltage-independent) reactions. For the electrogenic $Cl^-$ pump in *Acetabularia* these four rate constants have been determined from electrical measurements of the current-voltage relationship of the pump (Gradmann, Hansen & Slayman, 1981; *in:* Electrogenic Ion Pumps, Academic Press, New York). The unidirectional $Cl^-$ efflux through the pump can also be calculated by the availiable reaction kinetic parameters. $^{36}Cl^-$ efflux experiments on single *Acetabularia* cells with simultaneous electrical stimulation (action potentials) and recording, demonstrate the unidirectional $Cl^-$ efflux to depend on the membrane potential. After subtraction of an efflux portion which bypasses the pump, agreement is found between the measured flux-voltage relationship and the theoretical one as obtained from the reaction kinetic model and its parameters from the electrical data.

**Key words:** *Acetabularia*, $Cl^-$ flux, current-voltage relationships, electrogenic pump, ion-transport model, nonlinear kinetics

In recent studies [15, 10], a concept for the reaction kinetic treatment of "Class-I" models has been developed. Class-I comprises all transport systems with one pair of rate constants sensitive to the driving force under consideration, in this study the membrane potential $V$. This model allows curve-fitting of experimental data also in cases where not all of the intermediates of the transport cycle are known.

The application of this concept was successful in several cases. In *Neurospora* and *Acetabularia* it enabled the evaluation of rate constants in the transport cycle of electrogenic pumps from measured current-voltage ($I-V$) curves and the description of the action of $CN^-$ or light [5]. In *Chara*, a mathematical treatment of the flux measurements on the basis of the Class-I model resulted in the determination of the binding order in a $2H^+/Cl^-$ co-transport system [17]. The effect of internal pH in *Neurospora* on transport activity fulfills exactly the prediction of the model (D. Sanders, U.-P. Hansen & C.L. Slayman, *in preparation*).

Our model, in its most simple version, consists of two "lumped" states of the carrier, one outside and one inside. The two states are linked by two pairs (forwards and backwards) of rate constants, the voltage-sensitive pair which describes the transition of charged particles from one side of the membrane to the other and a voltage-insensitive pair which summarizes the remaining reactions of the voltage-insensitive part of the ionophoric cycle (such as substrate binding to and dissociation from the carrier molecule, phosphorylation, dephosphorylation and transport of the electroneutral form of the carrier molecule). It should be noted that, according to a recent suggestion [12], the "carrier" does not physically have to move across the membrane; it just describes a transporting macromolecule in the mem-

* Institut für Angewandte Physik, Neue Universität, Haus N 61 A, D-2300 Kiel, West Germany.

** *Address for correspondence:* Max-Planck-Institut für Biochemie, Abteilung Membranbiochemie, D-8033 Martinsried, West Germany.

0022-2631/81/0062/0139 $02.00

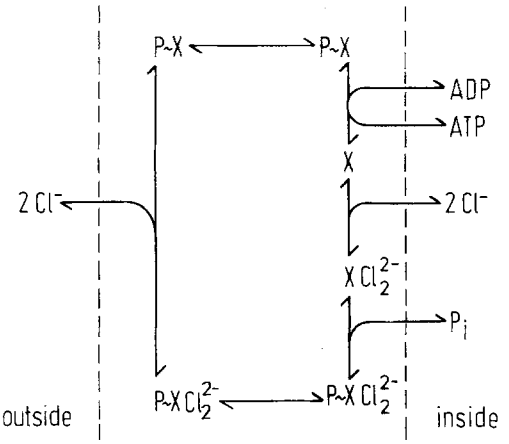


**Fig. 1.** Hypothetical reaction scheme for the electrogenic $Cl^-$ pump in *Acetabularia*; minimum of six different states and 12 rate constants. Rationale of details in text

brane which can react with substances on either side of the membrane during particular states of the transport cycle.

An explicit reaction cycle for the electrogenic $Cl^-$ pump in *Acetabularia* is shown in Fig. 1 with a minimum of six distinct states and twelve rate constants. There may be more intermediates; however, the concept of gross rate constants and "reserve factors" (*see* refs. [15, 10] and Appendix) allows the representation of real systems by models with fewer states. The scheme of Fig. 1 serves as a working hypothesis. In this form it is consistent with the following conditions:

1. The stoichiometry between actively transported $Cl^-$ and metabolic energy equivalents (probably ATP) is 2:1 [4, 5].

2. If the energy conversion takes place in one of the voltage-insensitive reactions, the shape of the $I-V$ curve of the electrogenic pump $i_p(V)$ predicts that this step is very fast and follows directly the transition of charge [5, 10]; in our scheme this reaction is a dephosphorylation, it could be any transient from a high- to a low-energy state.

3. The site of energy input (ATP binding) does, therefore, not reflect the main site of energy conversion into transport; the results from *Neurospora* [5] support this view.

4. Phosphorylation and dephosphorylation must take place inside.

5. As in the $(Na^+ + K^+)$-ATPase, only phosphorylated states are transported [11].

6. Because of Nos. 2 and 5, the carrier-substrate complex is charged and the unloaded carrier is neutral. Here we differ from a previous presentation [5], when no criteria were available.

7. Phosphorylation and $Cl^-$ dissociation inside cannot be interchanged because of the rapid dephosphorylation of $P\sim X\,Cl_2^{2-}$ inside.

Since this scheme represents a Class-I model with respect to the membrane voltage, its voltage characteristics can exactly be described by any convenient $n$-state model, e.g. by the above simple reaction scheme with only four rate constants (Fig. 2*A*).

Voltage-sensitivity could be demonstrated for the electrical current through the pump [3, 6] and for unidirectional $Cl^-$ efflux [13] in *Acetabularia*. If both phenomena are features of the same mechanism, the explicit model as drawn from the electrical analysis could predict the absolute values of the unidirectional efflux $\phi_p$, through the pump as well as its sensitivity $\phi_p(V)$ to the membrane voltage $V$. By means of our reaction kinetic analysis, good agreement is found between the measured $Cl^-$ efflux-voltage relationship $\phi_p(V)_m$ and the theoretical one $\phi_p(V)_{th}$, as calculated from the parameters obtained from the current-voltage relationship $i_p(V)$ of the pump.

## Materials and Methods

### *Materials*

Cells of *Acetabularia mediterranea* were cultured in Erdschreiber solution [1, 9]. For experiments, young cells without a cap were used because of their approximately cylindrical shape. The length varied from 20–40 mm, the diameter from 0.2–0.5 mm. In order to eliminate effects of circadian rhythm and to adapt the cells to defined medium for the experiments, the cells were kept for at least 3 days before the experiment under continuous light (3.2 W $m^{-2}$, Osram L65W/30) in artificial seawater (in mM: 461 $Na^+$, 10 $K^+$, 53 $Mg^{++}$, 10 $Ca^{++}$, 529 $Cl^-$, 28 $SO_4^{2-}$, 2 $HCO_3^-$, 10 Tris/HCl buffer, pH 8.0), which was used as external medium throughout the experiments.

### *Electrical Data*

We refer to original electrical data from previous work [3]. Briefly, in voltage-clamp experiments, voltage steps were applied until the clamp current reached a steady state. In this state, short (50 msec) and small ($\pm 5$ mV) voltage pulses $\Delta V$ were superimposed on the voltage step. The fast response of the clamp current $\Delta I$ after recharging the membrane capacity then yields the early slope conductance $g_m^o = \Delta I/\Delta V$ of the membrane at each membrane voltage: $g_m^o(V)$. The conductance $g_d^o(V)$ of the diffusion processes is known from other experiments (when the pump is inhibited by low temperature or metabolic inhibitors) and can be subtracted from $g_m^o(V)$ in order to obtain the desired conductance $g_p^o(V)$ of the pump alone.

After integration of $g_p^o(V)$ over the membrane voltage $V$, we obtain $i_p^*(V)$ of the electrogenic pump, where only the integration constant is missing. Since we know the equilibrium potential of the pump $E_p$ from the intercept of the steady-state current-voltage relationships of the membrane $i_m(V)$ under different metabolic

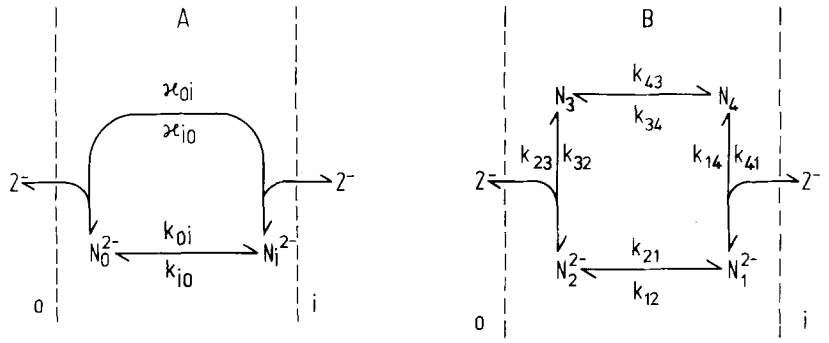


**Fig. 2.** Simplified reaction kinetic models for electrogenic $Cl^-$ pump in *Acetabularia*. *A*: two-state model: *B*: four-state model; parameter values in Table 1

conditions [3], we can determine the appropriate integration constant in order to obtain zero pump current at $E_p$. This yields the final $i_p(V)$.

### *Flux Measurements*

The methods for tracer flux experiments in *Acetabularia* are also given in previous studies [8, 13–15]. For washout experiments, cells fully equilibrated with $^{36}Cl^-$ in the external medium were mounted on a slanted plexiglass board which allowed continuous smooth rinsing of the cell with nonradioactive medium simultaneously with electrical stimulation and recording of the cell with conventional glass microelectrode techniques. Samples of the release of radioactivity from the cell to the washing medium have been taken in intervals of 15–600 sec. The lag time of the apparatus was about 3 sec. This has been accounted for in the temporal analysis of the flux data with respect to the immediate electrical recordings (Fig. 5).

For the evaluation of the washout experiments, a standard procedure [2] has been applied. However, conventional compartment analysis turned out to be inappropriate for *Acetabularia* [3, 13] and a useful mathematical treatment for the apparent three-compartment system (vacuole, cytoplasm and vesicles) is still missing. Therefore, we can only analyze flux "components" rather than physical compartments. The presented flux data of the particular components are just the area related products of the rate constants ($1/\tau$) times the contents, which can be obtained directly from the washout kinetics. We tend to assume that the high $Cl^-$ fluxes of component-1 may represent the plasmalemma fluxes out of an "inflated" (vesicles) cytoplasmic compartment [13].

Statistical data are presented as means of at least four samples ±SEM.

## Results

### *Model Parameters from Electrical Data*

The $i_p(V)$ data of the experiment for Fig. 3*B* have been obtained under bright white light ($10^3\,W\,m^{-2}$) from the $g_p^o(V)$ data (Fig. 3*A*). It has been shown [15, 10] that the two-state model shown in Fig. 2*A* is sufficient for the description of $I-V$ relationships of Class-I systems such as Fig. 1. The solid line in Fig. 3 is the result of fitting the data by the $I-V$ equation of the two-state model:

$$i = zFN\frac{k_{io}\kappa_{oi}-k_{oi}\kappa_{io}}{k_{io}+k_{oi}+\kappa_{io}+\kappa_{oi}}. \tag{1}$$

Equation (1) is identical to Eq. (A1) in the Appendix. In Eq. (1) the pseudo-two-state parameters are used which comprise the reserve factors, $r_1$ and $r_2$ in addition to the real two-state parameters:

$$k_{io}=k_{12}/r_1=k_{io}^o\exp(z\,u/2) \tag{2a, b}$$

$$k_{oi}=k_{21}/r_2=k_{oi}^o\exp(-z\,u/2) \tag{3a, b}$$

$$\kappa_{io}=\kappa_{12}/r_1 \tag{4}$$

$$\kappa_{oi}=\kappa_{21}/r_2. \tag{5}$$

Sensitivity to the membrane voltage $V$, enters Eq. (1) by Eqs. (2b) and (3b) by

$$u=VF/RT \tag{6}$$

with $R, T$ and $F$ having their usual meanings. The charge of the transportee is $z=-2$ for our application. $N$ is the total number of carrier molecules per surface area. The reserve factors $r_1$ and $r_2$ result from the unknown intermediates [*see* Eq. (A6b) in the Appendix]. On one hand they enable the mathematical treatment of partially unknown systems; on the other hand they render the estimation of the "real" rate constants (indexed by 1 and 2) from the pseudo-two-state rate constants (indexed by $i$ and $o$) rather difficult [10].

Fitting the data of Fig. 3*B* by Eq. (1) results in the parameter values for the two-state model (Fig. 2*A*) as listed in Table 1. (A minute discrepancy between the fitted curve in Fig. 3 and the measured $i_p$ values at $-114$ and $-104$ mV arises from the fact that jointly fitting of the data used here with dark $i_p(V)$ data (not shown here), obtained from the same cell, results in identical rate constants for both sets of data but with a smaller $N$ for the dark data [5].)

The fitting procedure can be carried out in a straightforward manner, because for the four desired parameters, four empirical parameters are available from the measurements: the two saturation currents yield the two $\kappa$ values; the equilibrium potential and the half-saturation voltage yield the $k^0$ values with known $\kappa$ values.

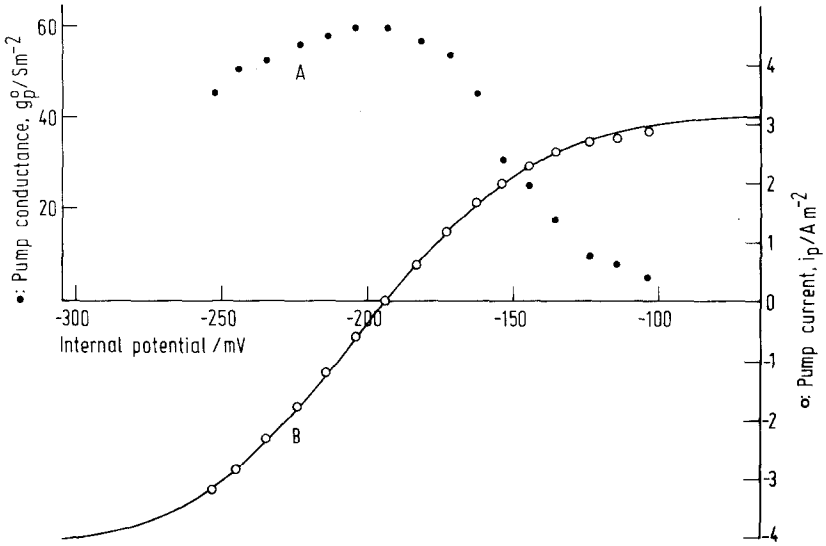


**Fig. 3.** Electrical steady-state characteristics of the electrogenic pump. (*A*) *solid symbols:* early slope conductance of the pump (membrane conductance minus a minor leak conductance) measured by voltage clamp; data from ref. [3]. (*B*) *open symbols:* pump current as determined by integration of the conductance data after correction for the leak; details in text. *Solid line:* fitted curve for the current data using two-state formalism [Fig. 2*A* and Eq. (1)]; conditions in text; parameter values in Table 1

**Table 1.** Parameter values for reaction kinetic two-state model for the electrogenic $Cl^-$ pump in *Acetabularia*, obtained from fitting data of Fig. 3 by Eq. 1; reaction scheme in Fig. 2*A*

| Two-state model parameters |
|---|
| $k_{io}^o = 4.8 \times 10^{-1}\ \text{sec}^{-1}$ |
| $k_{oi}^o = 3.4 \times 10^{6}\ \text{sec}^{-1}$ |
| $\kappa_{io} = 1.6 \times 10^{3}\ \text{sec}^{-1}$ |
| $\kappa_{oi} = 2.1 \times 10^{3}\ \text{sec}^{-1}$ |
| $N \equiv 10^{-8}\ \text{mol m}^{-2}$ |
| $z = -2$ |

Fits with $z=-2$ turned out to be better than with $z=-1$. In addition, the value of $E_p$ around $-200$ mV points also to a stoichiometry of 2:1 between the charge of the transported particle and a metabolic energy equivalent (ATP: about 400–500 mV).

### *Flux Measurements*

*Steady state.* In contrast to other work [15, 16], we find under steady-state conditions two clearly distinct components in the efflux kinetics, ignoring the additional one from the cell wall. Fig. 4 shows an example. Average data from influx and efflux experiments are given in Table 2. The good agreement between the influx and the efflux data confirms the reliability of the measurements.

At 4° C, including 24-hr incubation, the flux of the slow component is reduced (influx *ca.* 50%, efflux *ca.* 30%) compared to the control value from 21° C. In addition, in the cold, the internal $Cl^-$ concentration is also reduced and the flux of the fast component-1 has disappeared. This finding alone indicates that the fast component may be involved in the active $Cl^-$ uptake against the electrochemical gradient, which is equivalent to about $-170$ mV at 21° C and about $-100$ mV at 4° C after 24-hr incubation.

*Voltage-dependence.* In order to obtain the efflux as function of the membrane voltage, the $^{36}Cl^-$ release has been recorded during the slow (min) time course of electrically triggered action potentials. It could be demonstrated [4] that during an action potential in *Acetabularia* the early current-voltage relationship does not differ from the steady-state characteristics within the voltage range between the resting potential ($-170$ mV) and about $-100$ mV (for voltages more positive than $-100$ mV, time- and voltage-dependent permeability changes for $Cl^-$ and $K^+$ do occur during an action potential [7]). Therefore, the intended comparison of the steady-state early electrical characteristics with the efflux experiments is justified for the voltage range between the resting potential and $-100$ mV, even if for the flux data the voltage change is brought about by action potentials rather than by steady-state voltage clamp.

For evaluation of such efflux-voltage data (Fig. 5), the efflux during a sampling interval has been obtained from the release of $^{36}Cl^-$ related to the specific activity at the particular time of the washout kinetics, multiplying the efflux at time $t$ by the factor $\exp(t/\tau_1)$, where $\tau_1$ is the time constant of component-1. For each such efflux value the corresponding voltage was taken as the mean of the voltages at the beginning and the end of the particular

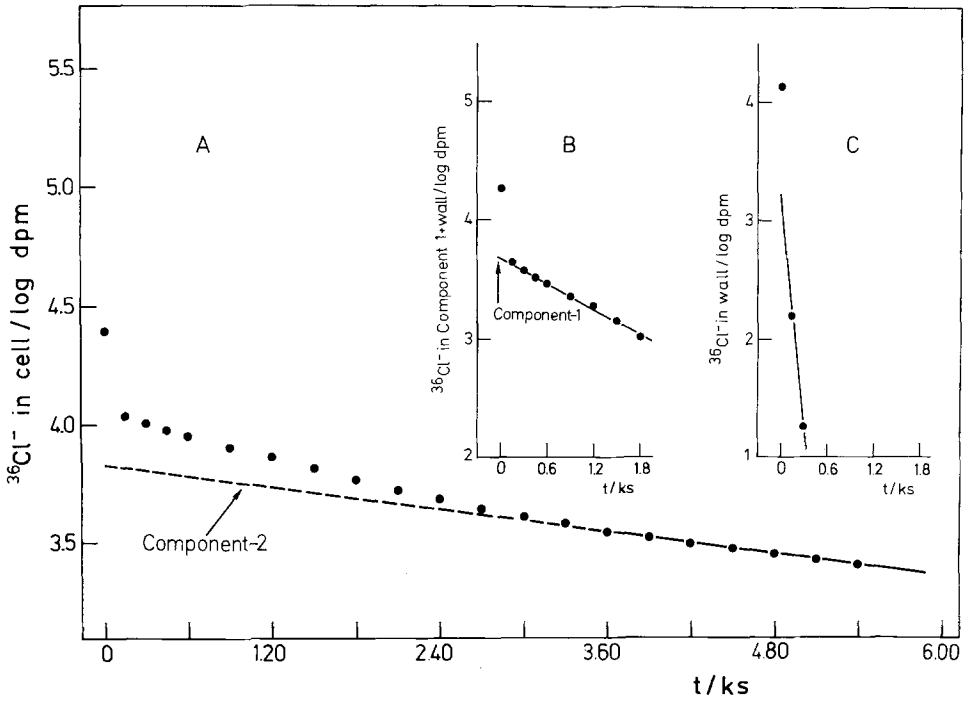


**Fig. 4.** Example for steady-state $^{36}Cl^-$ efflux kinetics of a fully labeled *Acetabularia* cell; 21° C, light. *A*: $^{36}Cl^-$ in cell after beginning of washout; parameters for component-2 taken from linear part of the slope by extrapolation to time zero. *B*: $^{36}Cl^-$ in cell minus component-2; parameters for component-1 taken from linear part of slope by extrapolation to time zero. *C*: $^{36}Cl^-$ in cell minus component-1 and component-2, reflecting cell wall compartment, which is not discussed in text

**Table 2.** Steady-state $Cl^-$ flux characteristics

| Flux characteristics | Component 1 | Component 2 | One component |
|---|---|---|---|
| | (21 °C; 412 ± 53 mM total conc.) | | 4° C; 24.8 ± 27 mM total conc. |
| Influx | $n=43$: | | $n=17$: |
| Time constant ($ks$) | 1.50 ± 0.16 | 12.24 ± 2.52 | 49.69 ± 5.40 |
| Content (% of total) | 50 | 50 | 100 |
| Flux ($\mu mol\, m^{-2} s^{-1}$) | 17.40 ± 4.1 | 1.46 ± 0.25 | 0.73 ± 0.07 |
| Efflux | $n=10$: | | $n=10$: |
| Time constant ($ks$) | 1.12 ± 0.09 | 9.72 ± 1.08 | 33.12 ± 4.32 |
| Content (% of total) | 47 ± 3 | 53 ± 3 | 100 |
| Flux ($\mu mol\, m^{-2} s^{-1}$) | 17.27 ± 0.21 | 2.30 ± 0.47 | 0.79 ± 0.14 |

sampling interval. For more than 90% of the measurements the change in potential was slower than 4 mV $sec^{-1}$. Therefore, with a temporal resolution of 0.5 sec (dropping rate), the related potential is determined with an accuracy of 2 mV.

Also for these flux-voltage data, in the range between resting potential and about −100 mV, no significant difference has been observed whether the data are taken from the de- or repolarizing phase (again in contrast to the voltage range more positive than −100 mV). By this finding, time-dependence must be excluded in favor of a genuine voltage-dependence.

For the synopsis of these results (Fig. 6), the pairs of data have been arranged in groups with respect to the voltage (10-mV intervals) and the corresponding flux values have been averaged. Since for the apparent value around −190 mV (−185 to −194 mV) only voltages between −185 and −189 mV were available, the real corresponding flux data for −190 mV are expected to be even higher.

In Fig. 6, the high $Cl^-$ efflux of component-1,

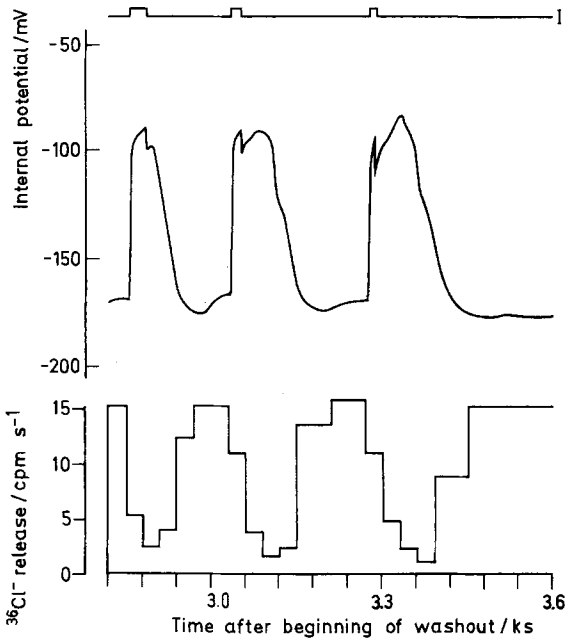


**Fig. 5.** Example for changes of $^{36}Cl^-$ release during electrically triggered action potentials; data are corrected for decrease of internal specific activity. Efflux values are calculated from these changes of $^{36}Cl^-$ release, related on prior steady-state $Cl^-$ efflux measurements. *I:* action potential triggering current pulses, 10 μA intracellular

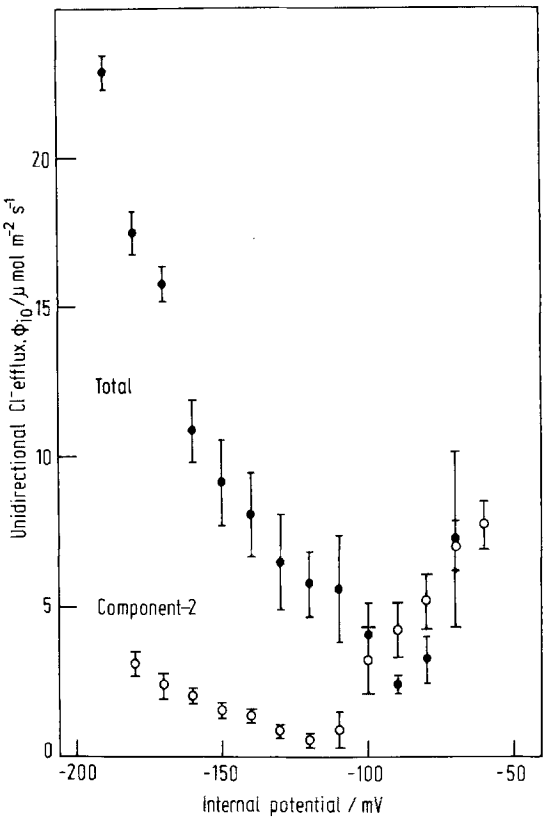


**Fig. 6.** Voltage-dependence of unidirectional $Cl^-$ efflux from entire cell (solid symbols: data from first two time constants of component-1) and from component-2 (open symbols: data from more than 9 ks after beginning of washout). Four-23 measurements per point

which dominates during the fast phase of the washout, shows a decrease with depolarizations from the resting potential down to about −100 mV before it increases again.

The low $Cl^-$ efflux, recorded 9 ksec and more after the beginning of the washout shows a similar dependence. This steady-state efflux of component-2 is, of course, lower than for component-1 (*see* Table 2). However, the voltage-stimulated increase for voltages more positive than −100 mV is about the same for both components.

From such $\phi(V)$ data three phenomena can be studied:

1. During an action potential, huge bursts of $Cl^-$ efflux (peak values around 60 μmol $m^{-2}$ $sec^{-1}$) can be observed. These have explicitly been described elsewhere [8] for light-triggered action potentials. They also occur with electrically triggered ones [13]. Probably they reflect release of NaCl vesicles, since they are electrically "silent" and $Na^+$ efflux bursts of comparable size have also been recorded during action potentials [13].

However, there is no strict correlation between action potentials and these $Cl^-$ efflux bursts. Occasionally they can occur without an action potential and action potentials can take place without these bursts. For the sake of simplicity, we selected those results for this presentation, which did not show these $Cl^-$ efflux bursts during an action potential.

2. The common increase of the $Cl^-$ efflux in both components for voltages more positive than −100 mV is paralleled by a corresponding increase of the membrane conductance. It has been shown to be involved in the mechanism of the action potential [7].

3. The drastic voltage-dependent decrease of the $Cl^-$ efflux between the resting potential and about −100 mV is obviously a feature of the high $Cl^-$ efflux. The measurements during the first two time constants of the fast component (2–4 ksec) of the washout contain both efflux components. In order to obtain the component-1 alone, we have to subtract component-2. After this subtration we obtain $\phi(V)$, which is the main subject of our comparison between unidirectional $Cl^-$ efflux and the electrical pump current.

With an explicit theory for our three-compartment system still lacking, it is an open question, whether the apparently similar voltage-dependence of component-2 reflects an additional voltage-sen-

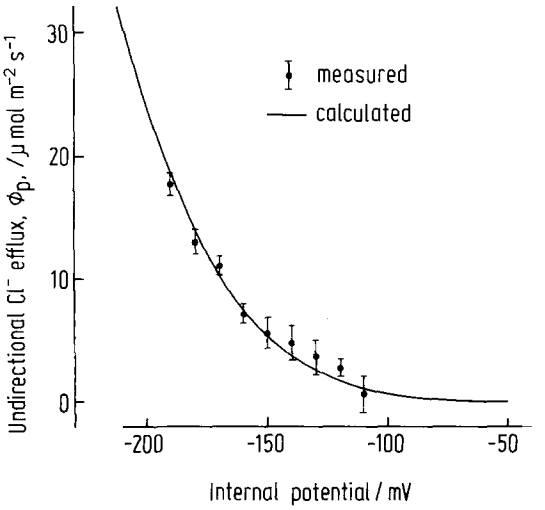


**Fig. 7.** Voltage-dependence of unidirectional $Cl^-$ efflux, $\phi_p(V)$, through pump pathway. Measured data: component-1 minus a portion of 2 µmol $m^{-2}$ $sec^{-1}$ bypassing the pump, corrected for a conducting $Cl^-$ leak of 100 mS $m^{-2}$. Calculated curve according to Eq. (8) and parameter values from Table 1; $N = 1.67 \times 10^{-8}$ mol $m^{-2}$

sitive process or the voltage-sensitivity of component-1.

*Fluxes Passing and Bypassing the Pump*

For the comparison of the electrical data with the $Cl^-$ flux measurements, we have to consider only that portion of the total efflux which is expected to leave the cell via the pump pathway. This portion can be estimated by subtracting the $Cl^-$ efflux remaining with the pump not operating. This $Cl^-$ efflux turned out to be 0.79 µmol $m^{-2}$ $sec^{-1}$ at 4° C (*see* Table 2); however, the internal $Cl^-$ concentration at 4° C is only about 60% of the control value (Table 2) and the bypassing flux will be larger anyway at normal temperatures. So the efflux bypassing the pump might be about 2 µmol $m^{-2}$ $sec^{-1}$ under normal conditions, which is about equivalent to the efflux of component-2 at 21 °C (*see* Table 2).

It should be mentioned that the major part of this $Cl^-$ efflux is electrically "silent". The passive $Cl^-$ conductance is only about 100 mS $m^{-2}$ [3]. After correction of the measured $\phi(V)$ by the above criteria, a $Cl^-$ efflux, $\phi_p(V)_m$, results which is supposed to be the $Cl^-$ efflux through the pathway of the electrogenic $Cl^-$ pump. Fig. 7 shows the results of $\phi_p(V)_m$.

## Discussion

The central question concerns the compatibility of the electrical data and the flux measurements, in particular the validity of the reaction kinetic scheme for the electrogenic $Cl^-$ pump in *Acetabularia*.

The experimental data of $\phi_p(V)_m$ must now be compared with the unidirectional $Cl^-$ efflux, $\phi_p(V)_{th}$, as predicted from the reaction kinetic scheme of the electrogenic pump (Fig. 1) and the numerical data from the electrical experiments (Table 1). In order to formulate this unidirectional efflux in reaction kinetic terms we start with the explicit scheme of Fig. 1. Here $\phi_p$ involves four reactions from $X$ inside to $P \sim X$ outside in counterclockwise direction. The explicit rationale for calculations of unidirectional fluxes in reaction kinetic terms is given in the Appendix. This approach has already turned out to be rather successful for the analysis of $Cl^-$ transport in *Chara corralina* [17].

It could be demonstrated [10] that for the scheme in Fig. 1, the two reactions between $P \sim X$ $Cl_2^{2-}$ outside and $XCl_2^{2-}$ inside can be described by only one pair of (voltage-sensitive) rate constants, $k_{12}$ and $k_{21}$ (*see* Introduction). Furthermore, we can also summarize the two pairs of rate constants between $X$ inside and $P \sim X$ outside in only one pair of rate constants, $k_{34}$ and $k_{43}$, because neither $V$ nor $Cl^-$ are involved in these reactions. Therefore, the four-state model of Fig. 2*B* should be appropriate for the calculation of $\phi_p(V)_{th}$.

For this mathematical treatment of the unidirectional flux, we have to trace the transportee from association inside to association outside via the $k_{12}$, $k_{21}$ rate constants, for the comparison with the electrical data. As the recycling of the carrier has to be incorporated also, we have four functions which have to be represented by a four-state model, as shown in Fig. 2*B*.

The calculation of the efflux starts from the obvious consideration that every conversion of state 4 into state 3 via states 1 and 2 results in the export of 2 $Cl^-$. The efflux is proportional to the concentration of state 4, $N_4$, and the gross rate constant[1] $\kappa_{4123}$, in which the numbering of the indices represents the sequence of involved states, in the four-state model in Fig. 2*B*.

$$\phi_{ex} = \phi_p(V) = n N_4 \kappa_{4123} = n N_4 \frac{k_{41} k_{12} k_{23}}{k_{12} k_{23} + k_{14} k_{23} + k_{21} k_{14}}. \quad (7a, b)$$

$n$ is the stoichiometry factor. In Eq. (7b), $\kappa_{4123}$ is given explicitly in terms of the four-state model of Fig. 2*B*. Voltage-sensitivity enters Eqs. (6a) and (6b)

[1] The principle of calculating gross rate constants by elimination of an intermediate $b$ between two states $a$ and $c$ is: $\kappa_{abc} = k_{ab} k_{bc}/(k_{ba} + k_{bc})$ and $\kappa_{cab} = k_{cb} k_{ba}/(k_{ba} + k_{bc})$.

via $k_{12}$ and $k_{21}$ by means of Eqs. (2b) and (3b).

In the Appendix, $N_4$ (which itself is voltage-dependent because of the redistribution of carrier with a change in $V$), is replaced by the constant total carrier $N$, and the pseudo-two-state rate constants $k_{io}$, $k_{oi}$, $\kappa_{io}$ and $\kappa_{oi}$ are introduced. The result (Eq. A17b) shows, in addition to the pseudo-two-state terms, some pseudo-four-state terms which cannot be replaced by pseudo-two-state terms. This means that different effluxes may exist for one $I-V$ relationship. This discrepancy arises from exchange fluxes, which do not show up in the net flux (current) but in unidirectional fluxes.

However, there are cases, in which efflux can be described completely by two-state parameters. For instance, if there is very rapid binding and release of the transportee, Eq. (A17b) converts to

$$\phi_p=\phi_{ex}=nN\frac{k_{io}(k_{oi}+\kappa_{oi})}{k_{io}+k_{oi}+\kappa_{io}+\kappa_{oi}}. \tag{8}$$

Curve-fitting of the efflux measurements shows that with $n=2$, Eq. (8) gives very good fits. In Fig. 7 the measured efflux data, $\phi_p(V)_m$ are fitted by Eq. (8). The peculiarity is that for the smooth curve the kinetic data of Table 1 are used and without utilizing those which would arise from a computer fit of the efflux data. As the data in Table 1 originate from electrical experiments, the fit in Fig. 7 proves that the same set of kinetic data accounts for the electrical and the flux measurements. The curve shape can be predicted from the electrical data with a high degree of accuracy, as shown in Fig. 7.

For a given total $N=10^{-8}$ mol m$^{-2}$ [5], the resulting absolute fluxes turned out to be somewhat smaller than the experimental data in Fig. 7
Agreement between the absolute values of the measured and the calculated $\phi_p$ in Fig. 7 has been achieved by a simple upscaling of the calculated curve by a factor of 1.7, which is equivalent to $N=1.7\times10^{-8}$ mol m$^{-2}$. This factor is within the statistical limits, since the used electrical data are taken from a single cell with a 1.6-fold smaller (pos.) saturation current than average (F. Tittor, *unpublished data*).

The above analysis on the basis of the theory of Class-I models results in several statements which are listed below. However, there is one statement which requires some extra comments. The treatment has shown very convincingly that the conductivity $g_p^o(V)$ has to be attributed to the electrogenic pump. In a previous study [3], the electrical response of the pump has been formally described by an electrical analog, which accounted for the observation of at least two time constants, a small one, in the range of msec (early event) and a large one, in the range of 10 sec (late event). In this analog, $g_p^o(V)$ "sees" only about 10% of the membrane potential, if the analog would be taken literally. By this treatment the $I-V$ curve becomes very steep and the physical meaning for such strong voltage-dependences (half saturation voltage about 3 mV) of a physiological transport system remains very problematic. Furthermore, the high measured $Cl^-$ fluxes could not be explained in terms of the electrogenic pump.

Equivalent circuits are very convenient and illustrative. However, they only account for linear properties. Since our currents and fluxes under consideration are clearly nonlinear functions of the voltage, they cannot be interpreted correctly by an equivalent circuit. On the other hand, the reaction kinetic analysis used here, is an appropriate treatment also for nonlinear systems such as the electrogenic $Cl^-$ pump in *Acetabularia*.

### *Conclusions*

The successful fit of the efflux data by kinetic parameters of the electrical data has several consequences:

1. The concept of Class-I models again turned out to be a powerful for describing ion transport in biomembranes.

2. The electrogenic pump in *Acetabualria* is a $Cl^-$ pump. The main part of the voltage-dependent $Cl^-$ efflux is the backflow through the pump (the main direction of flow is uptake).

3. Eq. (8) (Eq. A21) could be used instead of Eq. (A17). This implies that binding and release of the transportee ($Cl^-$) are very fast reactions [*see* Eq. (A19)]. This merges the binding and release of the transportee formally into the voltage-sensitive translocation (ideal "Mitchellian" behavior; *see* [10]), as in the case of the proton pump in *Neurospora*.

This work was supported by research grants from the Deutsche Forschungsgemeinschaft. We thank Dr. Dale Sanders for helpful discussion and critical reading of the manuscript.

## Appendix

### *The Relationship between Net Current Flow and Unidirectional Efflux of the Transportee in a Class-I Model*

It has been shown previously [5, 10] that all $I-V$ curves originating from reaction schemes with exactly one voltage-sensitive pair of rate constants ($k_{12}$ and $k_{21}$) sensitive to membrane potential (Class-I models) can be described by

$$I = zFN\frac{k_{io}\kappa_{oi} - k_{oi}\kappa_{io}}{k_{io}+k_{oi}+\kappa_{io}+\kappa_{oi}} \tag{A1}$$

with

$$k_{io}=\frac{k_{12}}{r_1},\quad k_{oi}=\frac{k_{21}}{r_2},\quad \kappa_{io}=\frac{\kappa_{12}}{r_1},\quad \kappa_{oi}=\frac{\kappa_{21}}{r_2}. \tag{A2a, b, c, d}$$

The symbol "$k$" represents elementary rate constants, whereas "$\kappa$" is used for gross rate constants as explained below. Voltage-sensitivity is assigned to the $k$ rate constants by

$$k_{12}=k_{12}^o \exp(zFV/2RT),\quad k_{21}=k_{21}^o \exp(-zFV/2RT). \tag{A3a, b}$$

$z$, $F$, $R$, $T$ and $V$ have their usual meanings. The factor 1/2 in the exponent originates from the assumption of the potential peak being in the middle of the membrane [12]. However, this is of no importance for the conclusions drawn in this article.

The peculiarity of the Class-I model is found in Eqs. (A2a) to (A2d). The rate constants labeled 1 and 2 are related directly to the elementary rate constants of the "real" model. $k_{12}$ and $k_{21}$ are elementary rate constants themselves, whereas $\kappa_{12}$ and $\kappa_{21}$ are gross rate constants lumping all the neutral reactions between state 1 and state 2. In case of the four-state model shown in Fig. 2*B*, $\kappa_{12}$ is the gross rate constant describing the conversion of state 1 into state 2 via states 4 and 3. Under steady-state conditions, $\kappa_{12}$ can be calculated from the elementary rate constants of the neutral limb, $N_1 - N_4 - N_3 - N_2$:

$$\kappa_{12}=\kappa_{1432}=\frac{k_{14}k_{43}k_{32}}{k_{41}k_{34}+k_{32}(k_{41}+k_{43})}=\frac{k_{14}k_{43}k_{32}}{D_1}. \tag{A4a, b}$$

$D_1$ is defined by the comparison of Eqs. (A4a) and (A4b); it is an abbreviation for the denominator. More than two indices are used for the rate constants, if the intermediate states are to be indicated. Similarly, $\kappa_{21}$ of the four-state model is:

$$\kappa_{21}=\kappa_{2341}=\frac{k_{23}k_{34}k_{41}}{k_{41}k_{34}+k_{32}(k_{41}+k_{43})}=\frac{k_{23}k_{34}k_{41}}{D_1}. \tag{A5a, b}$$

Unfortunately, theory shows that the analysis of an $I-V$ curve does not present $k_{12}$, $k_{21}$, $\kappa_{12}$ and $\kappa_{21}$ but rate constants labeled by $i$ and $o$ (inside and outside) according to Eq. (A1). The $i, o$ rate constants are related to the 1, 2 rate constants by the "reserve factors" $r_1$ and $r_2$ [Eqs. (A2a) to (A2d)].

In the pseudo-two-state model of Fig. 2*A*, only state 1 and state 2 of the transport molecule show up, but it can be assumed that there are still other unknown states "in reserve", e.g. four additional states in the model in Fig. 1. This causes no severe problems when gross rate constants as $\kappa_{12}$ and $\kappa_{21}$ are calculated. The only effect of an undetected intermediate is that a rate constant may be a gross rate constant while it was considered to be an elementary one.

However, in order to derive an equation like Eq. (A1), the law of mass conservation has to be incorporated. For this purpose the total number of carriers $N$ has to include all states, the known $N_1$ and $N_2$ plus the unknown $N_j$

$$N = N_1 + N_2 + \sum_{j=3}^{n} N_j. \tag{A6a}$$

The trick of the Class-I model approach [5, 10] is to select a model in which all $N_j$ are related by constant factors to $N_1$ and/or $N_2$. In that case Eq. (A6a) turns into

$$N = r_1 N_1 + r_2 N_2 \tag{A6b}$$

with $r_1$, $r_2$, the "reserve factors", being unknown but constant during the experiment. In case of the measurement of an $I-V$ curve, $r_1$ and $r_2$ stay constant, if $N_1$ and $N_2$ are the states adjacent to the voltage-sensitive charge translocation [$k_{12}$, $k_{21}$, *see* Eq. (A3a, b)], and, consequently $\kappa_{12}$ and $\kappa_{21}$ comprise all the neutral states.

The purpose of this article is to compare the efflux of labeled transportee with the electrical current which corresponds to a net flow of the transportee. Fig. 1 shows that every conversion of state $X$ into state $P\sim X$ via $P\sim X$ $Cl_2$ results in the efflux of two ions of the transportee ($Cl^-$). For the calculation of this flux, the four-state model of Fig. 2*B* is convenient. (The theory of Class-I models allows the selection of the most "convenient" model [10].) $k_{12}$ and $k_{21}$ are always assigned to the charge transport, $k_{23}$ and $k_{32}$ describe discharging and loading of the transportee at the outside, whereas $k_{14}$ and $k_{41}$ comprise an energetic step in addition to discharging and loading. Thus $\kappa$ symbols ought to be used. However, $k$ symbols are preferred in order to distinguish these rate constants from the $\kappa$ rate constants which lump four-state rate constants together. The recycling of the carrier is given by $k_{34}$ and $k_{43}$, which, too, ought to be $\kappa$ rate constants.

The conversion of state 4 into state 1, which results in the efflux of two $Cl^-$ is given by the gross rate constant $\kappa_{4123}$, with the indices again naming the terminal and the intermediate states

$$\phi_{ex}=\kappa_{4123}N_4. \tag{A7}$$

$\kappa_{4123}$ can be calculated from the four-state rate constants [compare introduction of Eqs. (A4) and (A5)]:

$$\kappa_{4123}=\frac{k_{41}k_{12}k_{23}}{k_{12}k_{23}+k_{14}(k_{21}+k_{23})}=\frac{k_{41}k_{12}k_{23}}{D_2} \tag{A8a, b}$$

with $D_2$ being an abbreviation of the denominator in Eq. (8a).

$N_4$ is voltage-dependent and has to be replaced by $N$. From Fig. 2*B* the following relationship is obtained:

$$N_4=\frac{k_{14}N_1+\kappa_{234}N_2}{k_{41}+\kappa_{432}}=\frac{k_{14}(k_{32}+k_{34})N_1+k_{23}k_{34}N_2}{D_1}. \tag{A9a, b}$$

From the pseudo-two-state model in Fig. 2*A* the following relationship is obtained [5, 10]:

$$N_2=\frac{k_{12}+\kappa_{12}}{k_{21}+\kappa_{21}}N_1. \tag{A10}$$

Combining Eq. (A10) with Eq. (A6b) results in

$$N_1=\frac{(k_{21}+\kappa_{21})N}{r_1(k_{21}+\kappa_{21})+r_2(k_{12}+\kappa_{12})}=N\frac{k_{21}+\kappa_{21}}{D_3} \tag{A11}$$

$$N_2=N\frac{k_{12}+\kappa_{12}}{D_3}. \tag{A12}$$

Replacing $N_1$ and $N_2$ in Eq. (A9) by Eqs. (A11) and (A12) and inserting Eqs. (A9) and (A8b) into Eq. (A7) leads to

$$\phi_{ex}=k_{41}k_{12}k_{23}\frac{k_{14}(k_{32}+k_{34})(k_{21}+\kappa_{21})+k_{23}k_{34}(k_{12}+\kappa_{12})}{D_1D_2D_3}N \tag{A13}$$

By means of Eq. (A5), $\kappa_{21}$ can be extracted in Eq. (A13)

$$\phi_{ex}=k_{12}\kappa_{21}\frac{k_{14}/k_{34}(k_{32}+k_{34})(k_{21}+\kappa_{21})+k_{23}(k_{12}+\kappa_{12})}{D_2D_3}N \tag{A14}$$

Using the identity [compare the denominators of Eqs. (A8a) and (A8b)]

$$1-\frac{k_{23}k_{12}}{D_2}=\frac{k_{14}(k_{21}+k_{23})}{D_2} \tag{A15}$$

results in

$$\phi_{ex}=N\frac{k_{12}\kappa_{21}}{D_3}$$
$$\left(1+\frac{k_{14}(k_{32}+k_{34})(k_{21}+\kappa_{21})+k_{23}k_{34}\kappa_{12}-k_{14}k_{34}(k_{21}+k_{23})}{k_{34}D_2}\right). \tag{A16}$$

The replacement of $\kappa_{12}$ and $\kappa_{21}$ by means of Eqs. (A4a) and (A5a) shows that nearly all terms in Eq. (A16) cancel each other:

$$\phi_{ex}=N\frac{k_{12}\kappa_{21}}{D_3}\left(1+\frac{\kappa_{3214}}{k_{34}}\right)=N\frac{k_{io}\kappa_{oi}}{k_{io}+k_{oi}+\kappa_{io}+\kappa_{oi}}\left(1+\frac{\kappa_{3214}}{k_{34}}\right) \tag{A17a, b}$$

with

$$\kappa_{3214}=\frac{k_{32}k_{21}k_{14}}{k_{21}k_{14}+k_{32}(k_{12}+k_{14})}=\frac{k_{32}k_{21}k_{14}}{D_2} \tag{A18a, b}$$

being the gross rate constant describing the transition of state 3 into state 4 via the electrically charged states (backflow of unlabeled $Cl^-$ from outside), whereas $k_{34}$ gives the backflow of the unloaded, neutral carrier.

The ratio $\kappa_{3214}/k_{34}$ comprises terms of the four-state model which cannot be replaced by pseudo-two-state terms ($i, o$) only. That implies that there are different efflux-voltage curves for a given $I-V$ curve. The reason for this is that a net flux (current) can comprise exchange terms which cancel each other. Eq. (A17) comprises the obvious case that the efflux is a minimum for a given current, if recycling of the unloaded carrier ($k_{34}$) is much more rapid than that of the loaded carrier ($\kappa_{3214}$). In this case, $\phi_{ex}$ depends only on $i, o$-terms.

### *Assumption of Very Rapid Loading and Discharge of the Transportee*

Introducing the assumption

$$k_{14}, k_{41}, k_{23}, k_{32} \gg \text{others} \tag{A19}$$

into Eqs. (A5a) and (A18) results also in a form of $\phi_{ex}$ which is only dependent on $i, o$-terms:

$$\kappa_{21}=\frac{k_{23}}{k_{32}}k_{34} \quad \text{and} \quad \kappa_{3214}=\frac{k_{32}}{k_{23}}k_{21}. \tag{A20a, b}$$

Introducing Eqs. (A20a) and (A20b) into Eq. (A17) results in

$$\phi_{ex}=N\frac{k_{12}(\kappa_{21}+k_{21})}{r_1(k_{21}+\kappa_{21})+r_2(k_{12}+\kappa_{12})}=N\frac{k_{io}(\kappa_{oi}+k_{oi})}{k_{io}+k_{oi}+\kappa_{io}+\kappa_{oi}} \tag{A21a, b}$$

which, indeed, comprise only terms which can be obtained from $I-V$ curve measurements (Eq. A1). This is because the rapid loading and discharge reactions merge the binding of the transportee into the charge translocation step.

## References


1. Beth, K. 1953. Experimentelle Untersuchungen über die Wirkung des Lichtes auf die Formbildung von kernhaltigen und kernlosen *Acetabularia*-Zellen. *Z. Naturforsch.* **8b**:334–342
2. Cram, W.J. 1968. Compartmentation and exchange of chloride in carrot root tissue. *Biochim. Biophys. Acta* **163**:339–353
3. Gradmann, D. 1975. Analog circuit of the *Acetabularia* membrane. *J. Membrane Biol.* **25**:183–208
4. Gradmann, D. 1976. "Metabolic" action potentials in *Acetabularia*. *J. Membrane Biol.* **29**:23–45
5. Gradmann, D., Hansen, U.-P., Slayman, C.L. 1981. Reaction kinetic analysis of current-voltage relationships for electrogenic pumps in *Neurospora* and *Acetabularia*. *In:* Electrogenic Ion Pumps. C.L. Slayman, editor. *In:* Current Topics in Membranes and Transport. F. Bronner and A. Kleinzeller, editors. Academic Press, New York (*in press*)
6. Gradmann, D., Klemke, W. 1974. Current-voltage relationship of the electrogenic pump in *Acetabularia*. *In:* Membrane Transport in Plants. U. Zimmermann and J. Dainty, editors. pp. 131–138. Springer-Verlag, Berlin
7. Gradmann, D., Mummert, H. 1980. Plant action potentials. *In:* Plant Membrane Transport: Current Conceptual Issues. R.M. Spanswick, W.J. Lucas, and J. Dainty, editors. pp. 333–344. Elsevier/North-Holland Biomedical Press
8. Gradmann, D., Wagner, G., Gläsel, R.M. 1973. Chloride efflux during light-triggered action potentials in *Acetabularia mediterranea*. *Biochim. Biophys. Acta* **323**:151–155
9. Hämmerling, J. 1944. Zur Lebensweise, Fortpflanzung und Entwicklung verschiedener Dasycladaceen. *Arch. Protistenkd.* **97**:7–56
10. Hansen, U.-P., Gradmann, D., Sanders, D., Slayman, C.L. 1981. Interpretation of current-voltage relationships for "active" transport systems. I. Steady-state reaction-kinetic analysis of Class-I mechanisms. *J. Membrane Biol.* (*in press*)
11. Karlish, S.J.D., Yates, D.W., Glynn, I.M. 1978. Conformational transitions between $Na^+$-bound and $K^+$-bound forms of $(Na^+ + K^+)$-ATPase, studied with formycin nucleotides. *Biochim. Biophys. Acta* **525**:252–264
12. Läuger, P. 1979. A channel mechanism for electrogenic ion pumps. *Biochim. Biophys. Acta* **552**:143–161
13. Mummert, H. 1979. Transportmechanismen für $K^+$, $Na^+$ und $Cl^-$ in stationären und dynamischen Zuständen bei *Acetabularia*. Ph.D. Thesis, Universität of Tübingen, Germany
14. Mummert, H., Gradmann, D. 1976. Voltage dependent potassium fluxes and the significance of action potentials in *Acetabularia*. *Biochim. Biophys. Acta* **443**:443–450
15. Saddler, H.D.W. 1970*a*. The ionic relations of *Acetabularia mediterranea*. *J. Exp. Bot.* **21**:345–359
16. Saddler, H.D.W. 1970*b*. The membrane potential of *Acetabularia mediterranea*. *J. Gen. Physiol.* **55**:802–821
17. Sanders, D., Hansen, U.-P. 1981. Mechanism of $Cl^-$ transport at the plasma membrane of *Chara corallina* II. Transinhibition and the determination of $H^+/Cl^-$ binding order from a reaction kinetic model. *J. Membrane Biol.* **58**:139–153


Received 13 November 1980; revised 12 March 1981